Journal of Fiber Bioengineering and Informatics 6:1 (2013) 23–32
doi:10.3993/jfbi03201302

Bio-inspired Electrospun Fibre Structures - Numerical Model

Budimir Mijovic [a,*], Ante Agic [b]

[a] *Faculty of Textile Technology, University of Zagreb, Prilaz baruna Filipovica 28 a, 10000, Zagreb, Croatia*

[b] *Faculty of Chemical Engineering and Technology, University of Zagreb Marulicev trg 19, 10000, Zagreb, Croatia*

Abstract

A systems approach that integrates processing, structure, property and performance relations has been used in the design of multilevel-structured fibrous materials. For electrospun fibrous structure, numerical implementation of multiscale materials philosophy provides a hierarchy of computational models defining design parameters that are integrated through computational continuum mechanics. Electrospun micro/nano (multiscale) poly(ε-caprolactone) (PCL) fibrous scaffolds were studied. The fibrous structures were evaluated for their mechanical, morphological and cell attachment properties. The cell attachment studies showed that cell activity on multi-scale scaffolds was higher compared to micro-fibrous scaffolds. These results suggest that the combination of a micro- and nano-fiber hierarchical scaffold could be more beneficial for tissue engineering applications than for individual scaffolds.

Keywords: Electrospun PCL; Multiscale; Numerical Model

1 Introduction

The variety of materials and fibrous structures that can be electrospun allow for the incorporation and optimization of various nanofiber functions, either during spinning or through post-spinning modifications [1]. Electrospun nanofibers have more than ever received greater attention, primarily because nanoscaled structures can be easily fabricated by the simple electrospinning process. These non-woven structures show unique morphologies in nano- or micrometer scales according to various electrospinning conditions. The unique relationship between surface and mechanical properties that occurs at the nanoscale define features that form the basis of nanoscale fibres and their versatility [2-4]. The chemical interactions dominate at smaller scales while bulk mechanics at larger scales. The balance between them in the system is a determinant factor from the aspect of assembly, from shape to chirality to hierarchy. Complicated phenomena for fibrous structure operate at multiple material scales and are governed by varying degrees of network properties;

*Corresponding author.
Email address: bmijovic@ttf.hr (Budimir Mijovic).

thus, numerical models are a necessary tool to unravel the relationships among individual network components and the aggregate properties and functions of the whole system. For example, scaffold design structures, their fabrication and structural behaviour at different scales lead to numerous experimental and computational challenges. In particular, there is a need for modelling and test tissues at multiple scales to gain an insight into issues such as drug delivery, drug interaction and cellular–environment interactions. The modelling of bio-inspired materials, such as fibrous scaffold, involves the concepts of both forward and inverse modelling [5]. A forward problem is to simulate biological material properties and responses using internal microstructures already determined by nature. On the other hand, a bio-inspired design may be regarded as an inverse problem. Here the internal microstructures are not initially known and the aim is to design these structures that will provide the desired properties, which may be required to be superior to those of nature. An inverse problem is inherently difficult since the specified performance criteria might consist of multiple properties (high strength, high toughness, significant extensibility, etc.) and multi-physics properties (elastic stiffness, thermal conductivity etc.).

Learning from nature is a source of bio-inspiration for scientists and engineers to design multifunctional synthetic materials with multiscale structures. Hierarchical structures with extraordinary properties that exist are widespread in bio-systems, such as bone, skin, nacre (shell) etc. The lessons drawn from hierarchical biological materials could obviously help us to design new nanostructure engineering materials and products [6-8]. Hierarchy in a material system is represented by several structural quantifications. The first come from the multiscale nature, i.e., the system is built on different structural levels with gradual transition in sizes among them. This multiscale always brings multiple heterogeneity into the system where each phase occupies a relevant structure level. This current paper examines how such multi-scaling, hydrogenizing or multi-phasing are advantageous or beneficial to account for the associated unique functionalities in fibrous materials systems.

2 Hierarchical Nanofiber-based Structure

According to the present stage of technology [9], at least four different levels of organization (see Fig. 1) can be put together to form a nanofiber based hierarchically organized structure. At the first level (nanoscale), nanoparticles or a second polymer can be mixed in the primary polymer solution and electrospun to form composite nanofiber. With the incorporation of nano-objects into electrospun solution it is possible to create nanofibers with various properties such as conductive network, ultraporous fibers, and ultrastrong fabrics. Using a dual-orifice spinneret design, a second layer of material can be coated over an inner core material during electrospinning to create the second level organization. Rapid evaporation of the solvents during the spinning process reduces mixing of two solutions, thus forming core-shell nanofiber. Hollow nanofiber has many applications in drug transport, nanofluid devices, and nanofibre sensors. At the same level, various surface functionalization techniques may be used to introduce an additional property to the nanofiber surface. The third level organization is fibres oriented and organized to optimize structural performance. A multi-layered nanofiber fabric or mixed micro-nanofibers 3D structure can be fabricated *in situ* through selective spinning or using a multiple orifice spinneret design, respectively. There are various methods to produce a multiscale structure; one of them is to use modulation processing parameters during electrospinning and different setup constructions. Finally, the nanofibrous assembly may be integrated within a microfiber structure with various

processing techniques (laser ablation, photolithographic patterning) to create the fourth-level organization.

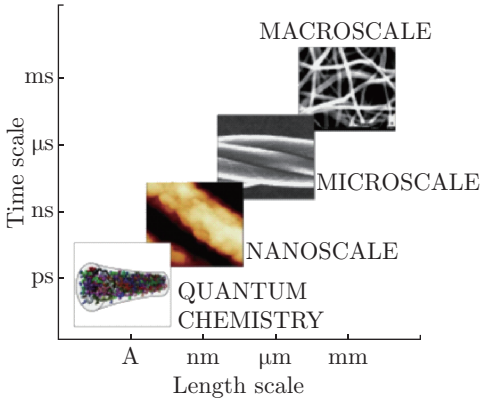

Fig. 1: Hierarchy levels of fibrous structure

3 Multiscale Structural Model

Hierarchical organization of the fibre structure introduces the need of multiscale approach in order to determine overall mechanical properties. Fig. 2 presents a SEM example of unimodal and modulated fibre structure with distinct micro and nanoscale morphology. The actual three-dimensional (3D) fibrous structure is described numerically by two scale models. Random nanofiber network on lower microscale creates a 3D membrane as a set of repeating representative volume elements (RVE). The mesoscale model is represented as a layered quasi-continuum 3D membrane between meso-fibre networks [10] (see Fig. 3).

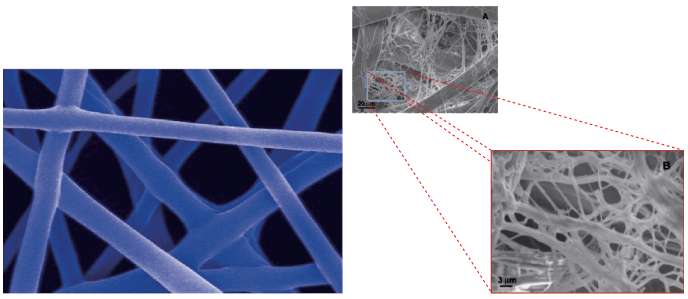

Fig. 2: SEM picture a) unimodal and b) bimodal fibre structure

3.1 Micro Level Problem

The nanofibre membrane model consists of finite set repeating (representative volume element) RVE in Gauss points. The network under RVE was derived from a marked two-dimensional random point field. The Poisson distribution for a large population was used as,

$$p(r) = \frac{\hat{n}}{r!} \exp(-\hat{n}) \tag{1}$$

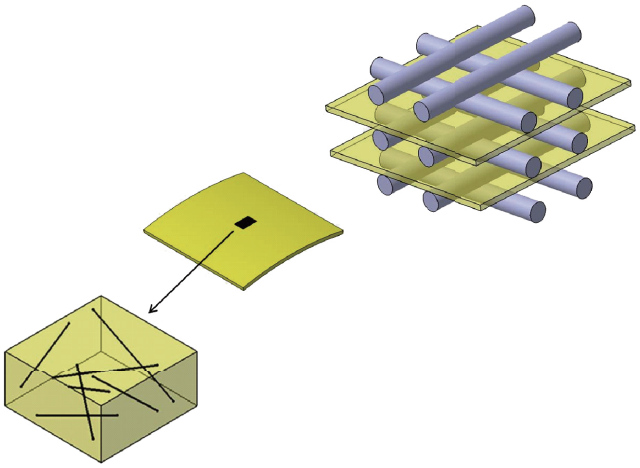

Fig. 3: Multiscale model fibrous structure

Eq. (1) represents the probability of finding r fiber centres per unit area for a network with a mean number of fiber centres per unit area of $\hat{n}$. Each point is associated with a length ℓ and orientation ϑ. Generally, the length probability density function used for the models construction is given by

$$p(\ell) = \frac{(\ell/b_1)^{b_2-1}}{b_1 \cdot (b_2 - 1)} \exp(-\ell/b_1) \qquad \hat{\ell} = b_1 \cdot b_2 \tag{2}$$

where, b_1 and b_2 are constants and l is the mean fiber length. The discrete nanofiber network is used in small regions of interest around the defects in the area of high strain gradients, whereas continuum models (membrane finite element with drilling degree of freedom) are used for the remaining domain of the nanofibre network.

3.2 Scale Transition

The basic principle of the method is highlighted in Fig. 4, where the scale transitions between micro and mesoscales are indicated. The model is based on solving two boundary value problems, one at each scale, using the finite element method. At the mesoscale, the domain is discretized into beam and membrane finite elements. The solution procedure on microscale follows the following steps:

a) The governing macroscopic kinematical quantities (the generalized strains, ε_m i.e. the membrane deformation and the curvature κ) are transferred to the micro-scale in order to define a boundary value problem on a micro-scale RVE. The equilibrium equation of the RVE in terms of the Cauchy stress tensor σ_m is

$$\nabla_m \cdot \sigma_m = 0 \tag{3}$$

where ∇_m is the gradient operator. (The subscript "M" refers to a macroscopic quantity, whereas the subscript "m" denotes a microscopic quantity). A node was placed at each interfiber crossing and a straight Timoshenko finite beam element was assigned to each connected fiber segment. Each bond was rigid and plastic shear deformation was not accounted for. The mechanical characterisations of the microstructural components are described by stress–deformation relationship for every nanofiber element. The micro-scale boundary value problem can be solved in a standard

manner, leading to a deformed RVE with boundary displacements and surface tractions [11-13] (see Fig. 4).

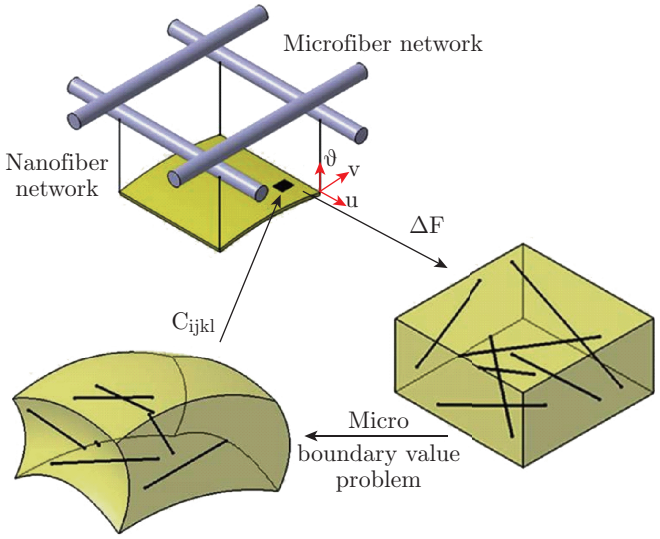

Fig. 4: The homogenization procedure for fibrous structure

b) Following the standard finite element procedure for the micro level RVE, after discretisation, the weak form of equilibrium (3) leads to a system of non-linear algebraic equations in the unknown nodal displacements u. The incremental microscopic system of equations, from which the dependent degrees u_P of freedom have been eliminated, is written and rearranged in the form

$$\begin{bmatrix} K_{PP} & K_{PF} \\ K_{FP} & K_{FF} \end{bmatrix} \cdot \begin{Bmatrix} \delta u_P \\ \delta u_F \end{Bmatrix} = \begin{Bmatrix} \delta f_P \\ 0 \end{Bmatrix} \tag{4}$$

System (4) is taken at the converged state of a microscopic increment, thus the residual forces in the free nodes u_F can be neglected $\delta f_F \approx 0$. Elimination of δu_F from the system (4) leads to the condensed tangent stiffness matrix $\hat{K}$ that relates the variations of

$$[\hat{K}] \cdot \{\delta u_P\} = \{\delta f_P\} \tag{5}$$

δf_P - is increment prescribed nodal forces. The tangents can be obtained directly from the RVE stiffness matrix through a static condensation process.

c) The stress distribution in the microscale is averaged, returning a macroscopic stress tensor Σ_M to every quadrate point in the mesoscale problem,

$$\Sigma_M = \frac{1}{V} \int_V \sigma_m dV \tag{6}$$

d) Convergence criteria for the stress are checked at the mesoscale.

Fig. 4 shows the schematic for this dual-scale methodology. It is emphasized that the scale-bridging is based on the homogenization technique, in which volume averaging theorems are applied to the microscale variables to determine the mesoscale ones.

3.3 Macroscopic Properties

From a macroscopic point of view, a (numerical) generalized stress–strain constitutive response at every macroscopic in-plane integration point is obtained. The energy averaging theorem, known in the literature as the Hill–Mandel condition [14] or macro homogeneity condition, requires that the macroscopic volume average of the variation of work performed on the RVE is equal to the local variation of the work on the macro scale.

$$\frac{1}{V}\int_V \sigma_m \cdot \delta F_m dV = \Sigma_M \cdot \delta F_M \tag{7}$$

The microfiber net was modelled as a combination of truss and beam elements. Nanofiber net is presented as a membrane finite element with drilling degree of freedom. The independent rotation field θ, for membrane element, is interpolated as follows [15]

$$\theta_z = \sum_{i=1}^{4} N_i(\xi,\eta)\cdot\theta_{zi} \tag{8}$$

And the in-plane displacement field vector $\{u,v\}^T$ is approximated by the Allman-type interpolation. The vibrational formulation suggested by Hughes [16] on macro scale is described as

$$\Pi(u,\gamma) = \frac{1}{2}\int_0^\ell \frac{M^2}{EI}dx + \frac{1}{2}\int_0^\ell \frac{N^2}{EA}dx + \frac{1}{2}\int_V \varepsilon_m^T D_m \varepsilon_m dV + \frac{1}{2}\gamma\int_V (\varepsilon-\vartheta)^2 dV + \int_V u^T f dV \tag{9}$$

The positive penalty parameter γ in equation (9) is problem-dependent. Minimization of Equation (9) results in a total matrix, as sums of beam/truss and membrane stiffness, as follows

$$K_{TOTAL} = K_{BEAM} + K_{MEMBRANE} \tag{10}$$

The stiffness matrix of the membrane has the following form

$$K_{MEMBRANE} = \int_V B_m^T D_m B_m dV + \gamma\int_V b^T b dV \tag{11}$$

where $[B]$ and $[D]$ are gradient displacement and elasticity matrix, respectively. The computations have been carried out using a finite element computer programme put together by the authors.

4 Experimental

The poly (ε-caprolactone) (PCL) solutions (Sigma–Aldrich, mol. weight = 65,000) in acetone were produced by stirring the solvent and particulate polymer at 50 °C until the solid was fully dissolved. Electrospun PCL fibers were produced using a 20 ml/h solution flow rate, a 10-20 kV potential between the needle tip and 10-20 cm collector distance. Samples were collected at room temperature and with humidity (≈30% RH). After deposition, the samples were exposed to a vacuum at room temperature for 8 h to insure that the residual solvent levels were insignificant. Characterization of the tissue scaffolds included image analysis, tensile tests, and porosimetry measurements to demonstrate enhanced properties and preferred morphologies.

5 Results

Fig. 5 shows an example of electrospun fabrics PCL structure in 2D and 3D form, where the 2D structure is represented as a thin shell that incorporates the 3D structure.

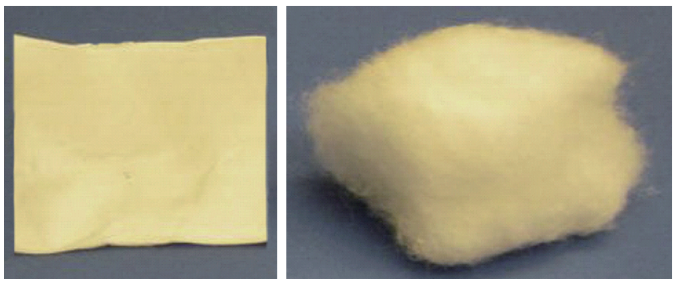

2D 3D

Fig. 5: 2 & 3D electrospun fibrous nanostructure

SEM photomicrographs of the PCL fibrous structure created with a cylindrical electrode is shown in Fig. 6. From the SEM photomicrographs it is evident that the fibre mat contains nano and micro fibres, which will be an ideal element for the fabrication of multifunctional fibrous structures.

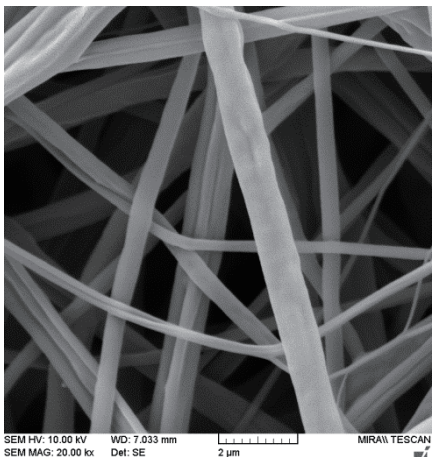

Fig. 6: SEM image of multiscale fibres of PCL

The experimental data for the fiber diameter dependence on solution concentration and electric field has been identified in previous works [17, 18]. The multiscale fiber distribution dependence on fibre diameter and electric field determined by multiple regression analysis using experimental data for electrospinning PCL solution is shown in Fig. 7. Based upon surface response methodology [19, 20] the coefficient in Weibull distribution model is given with Eq. (12),

$$f(x,y) = \frac{\beta_1}{\Theta_1}\left(\frac{x}{\Theta_1}\right)^{\beta_1-1}\exp\left[-\left(\frac{x}{\Theta_1}\right)^{\beta_1}\right] + \frac{\beta_2}{\Theta_2}\left(\frac{x}{\Theta_2}\right)^{\beta_2-1}\exp\left[-\left(\frac{x}{\Theta_2}\right)^{\beta_2}\right] \tag{12}$$

$$\beta_i = A_i \cdot y^2 + B_i \cdot y + C_i$$

$$\Theta_i = D_i \cdot y^2 + E_i \cdot y + F_i \quad i = 1, 2$$

where x and y are fibre diameter and electric field, respectively. An assumption that shapes parameter β and scale parameter quadratic depends on the electric field y. The surface contours plots of these parameters outline the optimum condition for electrospinning.

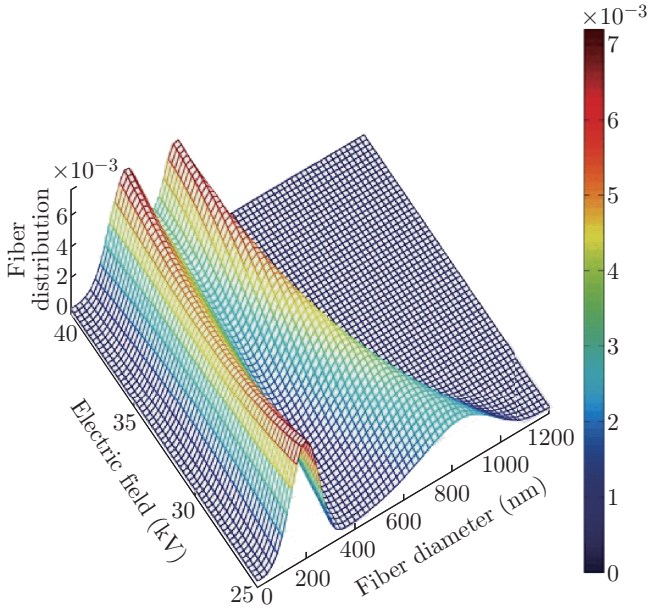

Fig. 7: Probability density dependence on fiber diameter and electric field

The computational model for elastic property was fit with the experimental stress–strain curve for a PCL electrospun mesh. The tensile properties of electrospun fabrics were measured as a function of fibre diameter and density, and compared to those predicted using a numerical model for fibrous networks previously described. The resultant best fit for the effective Young's modulus, was found to be dependent on fibre density and fibre diameter in Fig. 8.

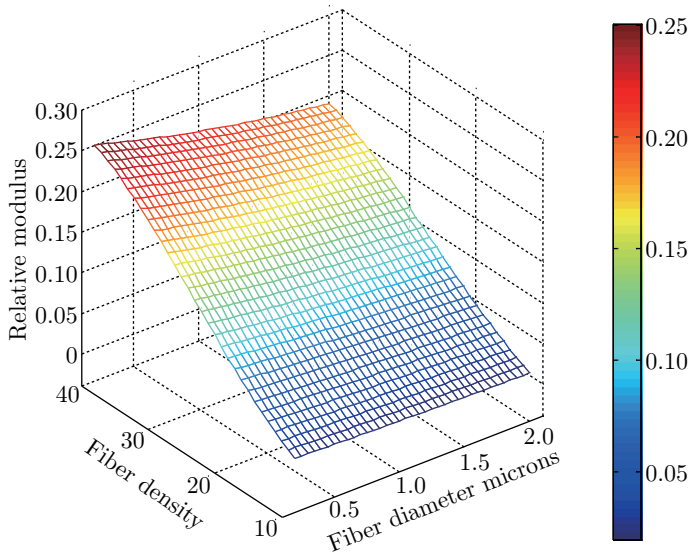

Fig. 8: Modulus dependence on fiber density and diameter

A common problem in the design of tissue engineered scaffolds using electrospun scaffolds is the poor cellular infiltration into the structure. To tackle this issue, cell adhesion on PCL electrospun

scaffold was investigated previously [21, 23]. The distribution of the electrospun fabric's pores was related to the average pore area, conducted by porosimetry [23].

6 Conclusion

The current study has successfully presented the nanofibrous membrane numerical model concerning finite element analysis, by solving two boundary value problems, one at each scale (transitions between micro and mesoscales). The mesoscale domain is discretized into beam and membrane finite elements, following the four steps solving the microscale level. The numerically generalized stress–strain constitutive response at every macroscopic in-plane integration point concerns the macroscopic scale and a computational model for the elastic property fitting with the experimental stress–strain curve of the electrospun PCL.

References

[1] Huang ZM, Zhang YZ, Kotak M, Ramakrishna S. A review on polymer nanofibers by electrospinning and their applications in nanocomposites. Composite Sci. Tech 2003; 63: 2223-2253.

[2] Xiuyan Li, RX, Yisong D, Yufang Z. Study on the Properties and Structure of Nano-TiO2 Modied Silk Fibroin Films. Journal of Fiber Bioengineering & Informatics 2011; 4: 155-164.

[3] Tao W, Wei Y, Li M. Condensed Structure of Regenerated Antheraea pernyi Silk Fibroin Porous Materials Prepared by Freeze-drying. Journal of Fiber Bioengineering & Informatics 2009; 2: 114-119.

[4] Li J, Li Y, Li L, Mak AFT, Ko F, Qin L. Preparation and biodegradation of electrospun PLLA/ keratin nonwoven fibrous membrane. Polymer Degradation and Stability 2009; 94: 1800-1807.

[5] Grinthal A, Kang SH, Epstein AK, Aizenberg M, Khan M, Aizenberg J. Steering nanofibers: An integrative approach to bio-inspired fibber fabrication and assembly. Nano Today 2011; 7: 35-52.

[6] Liu K, Jiang L. Bio-inspired design of multiscale structures for function integration. Nano Today 2011; 6: 155-175.

[7] Chen Y, Zhou S, Li Q. Microstructure design of biodegradable scaffold and its effect on tissue regeneration. Biomaterials 2011; 32: 5003-5014.

[8] Bechtle S, Fung S, Schneider GA. On the mechanical properties of hierarchically structured biological materials. Biomaterials 2010; 31: 6378-6385.

[9] Teo WE, Ramakrishna S. Electrospun nanofibers as a platform for multifunctional, hierarchically organized nanocomposite. Comp. Scie. and Tech 2009; 69: 1804-1817.

[10] Coenen EWC, Kouznetsova VG, Geers MGD. Computational homogenization for heterogeneous thin sheets. Int. J. Numerical Methods in Engrg. 2010; 83: 1180-1205.

[11] Srinivasan S, Jayakumar R, Chennazhi KP, Levorson EJ, Mikos AG, Nair SV. Multiscale Fibrous Scaffolds in Regenerative Medicine. Adv. Polymer. Sci. 2011; 12: 163-176.

[12] Agic A. Multiscale modeling electrospun nanofiber structure. Materials Science Forum 2012; 714: 33-40.

[13] Temizer I, Wriggers P. On the computation of the macroscopic tangent for multiscale volumetric homogenization problems. Comput. Methods Appl. Mech. Engrg 2008; 198: 495-510.

[14] Hill R. On constitutive macro–variables for heterogeneous solids at finite strain. Proc Royal Soc. London 1972; A326: 131-147.

[15] Bergan PG, Felippa CA. A triangular membrane element with rotational degrees of freedom. Computer Methods in Applied Mechanics and Engineering 1985; 50: 25-69.

[16] Hughes TJR, Brezzi F. On drilling degrees of freedom, Computer Methods in Appl. Mechanics and Engineering 1989; 72: 105-121.

[17] Agic A, Nikitovic M, Mijovic B. Design of dermal electrospun replacement, Periodicum Biologorum 2010; 112: 63-68.

[18] Mijovic, B., Agic. A. The effect of processing and rheological variables on the morphology of dermal electrospun scaffolds., Journal of Fiber Bioengineering & Informatics 2011; 3: 182-187.

[19] Hilpert M, Miller C. Pore-morphology based simulation of drainage in totally wetting porous media. Adv. Water Resourse 2001; 24: 243-255.

[20] Montgomery DC. Design and Analysis of Experiments: Response surface method and designs. John Wiley and Sons, Inc., New Jersey 2005.

[21] D'Amore A, Stella JA, Wagner WR, Sacks MS. Characterization of the complete fiber network topology of planar fibrous tissues and scaffolds. Biomaterials 2010; 31: 5345-5354.

[22] Mijovic B, Tominac M, Agic A, Zdraveva E, Bujic M, Špoljaric I, Kosec V. Study on cell adhesion detection onto biodegradable electrospun PCL scaffold. J. of Fiber Bioeng. & Informatics 2012; 5: 1-8.

[23] Soliman S, Sant S, Nichol JW, Khabiry M, Traversa E, Khademhosseini A. Controlling the porosity of fibrous scaffolds by modulating the fiber diameter and packing density. J Biomed. Mater. Res. Part A 2011; 96A: 566-574.